Simulation of the Dynamic and Equilibrium Properties of Many-Chain Polymer Systems

David E. Kranbuehl*

Department of Chemistry, The College of William and Mary, Williamsburg, Virginia 23185

Peter H. Verdier

National Bureau of Standards, Washington, D.C. 20234. *Received July 29, 1983*

ABSTRACT: Computer simulation of the motions of systems of lattice-model polymer chains on a simple cubic lattice was employed in order to study the effects of excluded volume and chain entanglement on the relaxation behavior and equilibrium properties of polymer chains. Multiple chains of from 8 to 64 beads each were studied, with periodic boundary conditions and with up to 80% of the lattice sites occupied. As chain concentration increased, equilibrium dimensions were found to approach random-walk values, in agreement with results obtained by previous workers. The long relaxation times inferred from the limiting long-time behavior of the autocorrelation functions for the end-to-end vector show a dramatic increase with increasing concentration. The variation of the long relaxation time with chain length and concentration is represented reasonably well by a simple free volume model and an additional chain-length-dependent factor.

Introduction

In the development of models for the dynamical behavior of random-coil polymer chains, the volume occupied by the chain elements and the resulting entanglements of the chain with itself and with other chains have proven extremely difficult to treat analytically. In particular, the bead–spring models introduced by Rouse[1] and Zimm,[2] which have achieved considerable success in describing the behavior of random-coil chains in dilute solution,[3,4] have not been amenable to inclusion of excluded volume and entanglement. Various pictures have been introduced to characterize these effects. The most recent and widely accepted of these is the "reptation" model, in which a chain in a nondilute solution is viewed as diffusing inside a randomly shaped tube formed by the surrounding chain segments.[5-11] The concentration at which diffusion in a tube begins and types of fluctuations in tube shape ("tube reorganization") which occur are among the questions which are not directly addressed. Thus one is left with ambiguous concepts of concentration regions where the behavior of the system goes from one set of model predictions to another.

An alternative, nonanalytical approach to the investigation of the dynamical behavior of polymer chains is computer simulation of Brownian motion of simple models of the chains. This approach allows the introduction of interactions which are not presently amenable to analytical treatment. In particular, the effects of volume exclusion and chain entanglement on equilibrium and dynamical behavior may be simulated directly.

Several simulation studies of the equilibrium properties of multichain systems have been reported.[12-18] These studies have provided insight into the power-law dependence of the square of end-to-end length $\langle l^2 \rangle$ on the number of segments $(N-1)$ in a chain: $\langle l^2 \rangle \sim (N-1)^{\delta}$. The decrease in δ from its dilute-solution value of about 1.2 in good solvents to a value near 1.0 in the melt phase has been observed. Current work is focused on how closely δ approaches unity in the melt.

In the past few years several simulation studies of the dynamical behavior of multichain systems have been reported.[19-23] The earliest of these[19] was a preliminary report on the effect of concentration upon the long-time relaxation properties. It was limited to relatively short chains, of 9 and 19 segments. Chain relaxation times were found to increase very rapidly with increasing concentration. More recent studies of long relaxation times have been limited to 16-segment chains,[21] to allowing only one chain to move in a matrix of "frozen" chains,[22] and to treating intra- and interchain effects differently.[23]

In the present paper, we report the results of simulation studies of the equilibrium and dynamical behavior of lattice-model chains of from 7 to 63 segments, at concentrations ranging from very dilute to near-melt. Multiple occupancy of lattice sites and motion of one chain through another are prohibited. We exhibit the dependence of chain dimensions, long relaxation times, and center-of-mass translational diffusion constants upon chain contour length and concentration.

Model

The dynamical lattice model of a linear polymer chain used in this work has been described in the original work of Verdier and Stockmayer[24] and expanded upon in later work.[25-29] A chain of $N-1$ steps is modeled by a set of N connected points, which we shall refer to as beads, on a simple cubic lattice, the connections lying along cube edges. Brownian motion of the chains is simulated by choosing a piece of a chain at random and then moving only this piece of this chain according to rules which maintain chain connectivity. Entanglement and excluded volume effects are introduced by not allowing beads to move to sites which are already occupied. This choice and (possible) movement process, which will be referred to as a bead cycle, is taken to represent $(CN)^{-1}$ units of time, where C is the number of chains in the system and N is the number of beads on each chain. As it is repeated again and again, each chain moves from one conformation to another, eventually (in principle) taking on all the conformations of its equilibrium ensemble. Repeated sampling of the state of the system then allows the construction of estimates of equilibrium ensemble averages of chain dimensions and of time-correlation functions and diffusion constants for the study of relaxation behavior.

In the present work we employ two kinds of local bead move, which we shall call one-bead and two-bead moves. Let the beads of a given chain be numbered consecutively along the chain from 1 to N and let σ_j be the vector from bead j to bead $j+1$. A one-bead move of bead j is carried out by interchanging σ_j and σ_{j-1}, moving only bead j in the process. In a similar way, a two-bead move of beads j and $j+1$ is carried out by interchanging σ_{j-1} and σ_{j+1}. For both kinds of move, if selection of a site near an end of the chain would result in one of the σ's being interchanged with a

0024-9297/84/2217-0749$01.50/0

nonexistent vector beyond the end of the chain, it is replaced by a vector chosen at random from the six possibilities for this lattice.

A bead cycle begins by making a random choice whether to attempt a one-bead move or a two-bead move. In the present work, the choice is made with equal probability for each. In the notation of ref 28 and 29, this corresponds to a value of the fraction p of two-bead moves of 0.5. Next, a chain and a location along the chain (a single bead for a one-bead move and a pair of connected beads for a two-bead move) are chosen at random. Finally, the selected move is attempted. If it would result in moving a bead to a site already occupied by another bead, either of the selected chain or of another chain, no move is made; if not, the chosen move is made. In either case, the bead cycle is completed and the process repeats with the selection of the type of move to be attempted in the next bead cycle.

For the present multichain studies, periodic boundary conditions were imposed, with a period of 16 lattice units in each direction. Thus the entire lattice space is divided into cubical subunits, 16 lattice units to a side, containing identical chain conformations. If a given chain conformation passes through a side of one subunit, it appears to reenter through the opposite side. Thus each chain in the simulations represents an infinite number of identical chains, separated by multiples of 16 lattice units in each direction. (A few comparison studies were carried out with a period of 32 instead of 16, to estimate the effects of finite period on the results.)

As in our previous work, relaxation of and from equilibrium states was examined. It was therefore necessary to generate initial random starting configurations for the simulations. For each system, defined by the number of chains and the number of beads in each chain, an initial, exceedingly nonrandom set of chain configurations was chosen in such a way as to guarantee no multiple occupancy of lattice sites. The move rules were then carried out until the squares of the end-to-end lengths of the chains appeared to be fluctuating about constant values. From this point on, as the simulations proceeded the end-to-end vector $\mathbf{l}$ and the coordinates of the center of mass were sampled for each chain in the system and used to form estimates of the averages $\langle \mathbf{l}(0)\cdot\mathbf{l}(t)\rangle$, $\langle l^2(0)l^2(t)\rangle$, and $\langle d^2(t)\rangle$, where the last quantity is the mean-square move of the center of mass of a chain in time t. These averages were then used to form estimates of the equilibrium quantites $\langle l^2\rangle$ and $\langle l^4\rangle$, the autocorrelation functions

$$\rho(\mathbf{l},\mathbf{l},t) = \langle \mathbf{l}(0)\cdot\mathbf{l}(t)\rangle / \langle l^2\rangle \quad (1)$$

and

$$\rho(l^2,l^2,t) = (\langle l^2(0)l^2(t)\rangle - \langle l^2\rangle^2)/(\langle l^4\rangle - \langle l^2\rangle^2) \quad (2)$$

and the translational diffusion constant

$$D = \langle d^2\rangle/(6t) \quad (3)$$

Results

Simulations were carried out for chains of 8, 16, 32, and 64 beads. For all but the 64-bead chains, simulations were carried out at eight values of the bead volume fraction ϕ, defined as the fraction of lattice sites occupied by beads. The numbers of chains were chosen to give values of ϕ spanning the range from 0.1 to 0.8. For the 64-bead chains, systems were studied at six values of ϕ, from 0.016 to 0.52. The total lengths of the simulations are shown in Table I in units of CN^3 bead cycles, where N is the number of beads on each chain and C is the number of chains in each lattice repeat unit of 16^3 points.

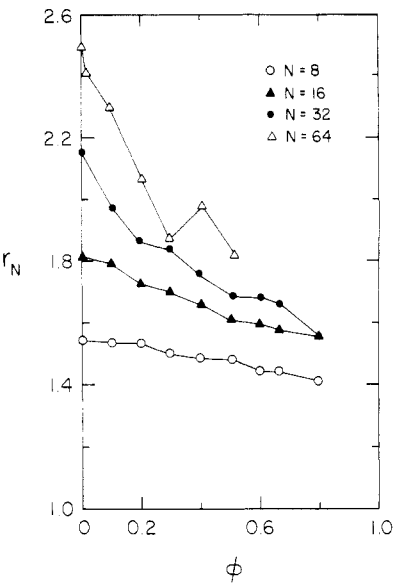

Figure 1. Ratios $r_N = \langle l^2\rangle/(N-1)$, where $\langle l^2\rangle$ is mean-square end-to-end length, for chains of N beads, vs. bead volume fraction ϕ.

Equilibrium Dimensions. Table I shows the mean-square end-to-end length $\langle l^2\rangle$, the mean fourth power $\langle l^4\rangle$, and the ratio $\langle l^4\rangle/\langle l^2\rangle^2$. Also shown for comparison are values of $\langle l^2\rangle$ for single-chain simulations, taken from ref 25. Since periodic boundary conditions were not employed in that work, these values correspond to $\phi = 0$. As ϕ increases, $\langle l^2\rangle$ gradually decreases, in agreement with results observed by others.[12-19] Figure 1 shows plots of $\langle l^2\rangle/(N-1)$ vs. ϕ. It will be seen that as ϕ increases toward 1.0, the values of $\langle l^2\rangle/(N-1)$ tend toward the values $3/2 - (5/8)[1-(1/5)^{N-1}]/(N-1)$ calculated[30] for a "5-choice" (i.e., self-reversal disallowed) random walk on a simple cubic lattice without excluded volume interactions, in agreement with earlier results obtained by Wall and Seitz.[13]

The power-law dependence of $\langle l^2\rangle$ on $N-1$ was estimated by fitting $\ln\langle l^2\rangle$ to a linear function of $\ln(N-1)$ by least squares at each value of ϕ. The resulting slopes δ are shown in Table II. As ϕ increases, they decrease from the dilute-solution value of about $^6/_5$ to 1.07 at $\phi = 0.8$.

Several studies[12-18] have examined the concentration dependence of δ for chains of lengths comparable with those employed in this work. The results have been extrapolated to the bulk-phase limit, where values of 1.04–1.07 are reported. Recently, equilibrium studies have been extended to chain lengths of 500 by Mansfield,[18] who reported a bulk-phase value of 1.03. All these studies support the conclusion that δ approaches the Flory Θ-temperature value of unity in the bulk phase, where self-repulsion of the chain segments is balanced by mutual repulsion of segments of neighboring chains.[31,32]

Relaxation Times and Diffusion Constants. Figure 2 shows semilogarithmic plots of the autocorrelation functions $\rho(\mathbf{l},\mathbf{l},t)$ for the end-to-end vector $\mathbf{l}$ vs. time t in units of CN^3 bead cycles for four typical systems. They are clearly not simple exponentials. However, after an intial rapid decay they all appear to approach limiting exponential behavior suggestive of a unique longest relaxation time τ_1. We have therefore extracted values of τ_1 by least-squares fitting each $\rho(\mathbf{l},\mathbf{l},t)$ to $a\exp(-t/\tau_1)$ in the region where $\rho < 0.6$. The resulting values of a and τ_1 are given in Table III, together with their standard deviations. Except for the case $N = 64$ and $\phi = 0.016$, the standard deviations were obtained by dividing the total length of each simulation into equal thirds, determining a and τ_1 separately from the sampled autocorrelation

Table I
Equilibrium Data for Chains on a Simple Cubic Lattice[a]

N	C	ϕ	T	$\langle l^2 \rangle$	$\langle l^4 \rangle$	$\langle l^4 \rangle / \langle l^2 \rangle^2$
8		0.000		10.8 (0.2)		
8	51	0.100	9.6	10.76 (0.10)	154.6 (2.7)	1.34
8	102	0.199	9.6	10.757 (0.016)	155.10 (0.37)	1.34
8	152	0.297	7.2	10.499 (0.083)	149.2 (2.0)	1.35
8	205	0.400	14.4	10.401 (0.027)	146.85 (0.70)	1.36
8	260	0.508	9.6	10.373 (0.061)	147.8 (1.4)	1.37
8	307	0.600	24.0	10.109 (0.034)	140.9 (1.1)	1.38
8	340	0.664	21.6	10.099 (0.032)	140.81 (0.52)	1.38
8	408	0.797	28.8	9.891 (0.059)	136.8 1.6)	1.40
16		0.000		27.2 (0.6)		
16	25	0.098	38.4	26.90 (0.22)	1023 (14)	1.41
16	51	0.199	19.2	25.90 (0.13)	959.8 (9.3)	1.43
16	76	0.297	24.0	25.51 (0.24)	933 (15)	1.43
16	103	0.402	14.4	24.92 (0.22)	894 (15)	1.44
16	129	0.504	16.8	24.18 (0.30)	850 (24)	1.45
16	153	0.598	16.8	23.93 (0.34)	841 (19)	1.47
16	170	0.664	28.8	23.64 (0.14)	822.5 (9.3)	1.47
16	204	0.797	43.2	23.33 (0.19)	797 (11)	1.46
32		0.000		66.7 (0.7)		
32	13	0.102	28.8	61.1 (2.0)	5546 (307)	1.49
32	25	0.195	14.4	57.8 (1.4)	4977 (204)	1.49
32	38	0.297	24.0	56.97 (0.73)	4879 (133)	1.50
32	51	0.398	14.4	54.55 (0.50)	4465 (82)	1.50
32	65	0.508	19.2	52.29 (0.77)	4188 (102)	1.53
32	77	0.602	37.2	52.09 (0.61)	4145 (85)	1.53
32	85	0.664	41.4	51.45 (0.36)	4042 (76)	1.53
32	102	0.797	46.3	48.22 (0.90)	3648 (155)	1.57
64		0.000		157 (3)		
64	1	0.016	345.6	151.7 (2.7)	33774 (1225)	1.47
64	6	0.094	57.6	144.7 (1.9)	31179 (940)	1.49
64	13	0.203	33.4	130.1 (2.4)	26114 (909)	1.54
64	19	0.297	18.7	118.0 (2.0)	21176 (481)	1.52
64	26	0.406	23.2	124.6 (2.0)	24145 (724)	1.56
64	33	0.516	23.0	114.5 (2.5)	20468 (969)	1.56

[a] N is the number of beads on each chain; C is the number of chains per 16^3 lattice sites; ϕ is the fraction of lattice sites occupied by beads; T is the total length of simulation, in units of CN^3 bead cycles, and $\langle l^2 \rangle$ and $\langle l^4 \rangle$ are the averages of the second and fourth powers of the chain end-to-end vectors. Values of $\langle l^2 \rangle$ for $\phi = 0$, shown for comparison, are taken from ref 25. Numbers in parentheses are sample standard deviations of the mean.

Table II
Values of δ Obtained by Fitting Values of the Mean-Square End-to-End Length $\langle l^2 \rangle$ of Chains of N Beads to the Form $\ln \langle l^2 \rangle$ = constant + $\delta \ln (N - 1)$ for Values of Bead Volume Fraction ϕ from 0 to 0.8

	ϕ								
	0	0.1	0.2	0.3	0.4	0.5	0.6	0.66	0.8
δ	1.22	1.18	1.13	1.10	1.13	1.09	1.10	1.09	1.07

function for each third and calculating the sample standard deveiations of the mean values of a and τ_1. For $N = 64$ and $\phi = 0.016$, the total simulation was divided into ninths rather than thirds.

In a similar way, relaxation times were also extracted from the autocorrelation functions $\rho(l^2,l^2,t)$ for the square of the end-to-end vector. The relaxation times so obtained typically ranged from one-sixth to one-third the corresponding values of τ_1, in agreement with results previously obtained[27] for isolated chains. In a general way, they appeared to parallel the variation of τ_1 with N and ϕ. However, as is clear from comparison of eq 1 and 2, the sampled values of the autocorrelation in l^2 are inherently much less precise than those of the autocorrelation in $\mathbf{l}$. As a result, the relaxation times obtained from the autocorrelation in l^2 are too imprecise for clear inferences to be drawn from their behavior.

Diffusion constants D of the centers of mass of the chains, calculated according to eq 3, are given in Table III. Also shown are the times T_D over which the displacements of the centers of mass were sampled and the ratios T_D/τ_1. Previous work[25,27] has shown that T_D needs to be much longer than τ_1 if $\langle d^2 \rangle/(6T_D)$ is to be an unbiased estimator of the macroscopic diffusion constant. Sampling times which are too short yield apparent diffusion constants which are too large. For the systems reported here it will be seen that T_D/τ_1 is not much larger than unity. Estimates of D obtained by sampling $\langle d^2 \rangle$ over times $T_D/2$ yielded values of D up to 20% larger than those given in Table III. Thus, these values of D tend to be systematically larger than the limiting long-time diffusion constants.

Table III also reports values of the dimensionless ratio $D\tau_1/\langle l^2 \rangle$. Previous work[27] has shown that for isolated chains this ratio is not sensitive to the presence or absence of excluded volume interactions. Although judgment must be hedged both by the knowledge of appreciable systematic errors in the values of D reported here and by the presence of considerable scatter, the ratios $D\tau_1/\langle l^2 \rangle$ do not appear to be very sensitive to the interchain interactions which increase with increasing ϕ, except possibly for the 8-bead chain systems, where $D\tau_1/\langle l^2 \rangle$ appears to decrease with increasing ϕ.

Finally, Table III shows the ratios T/τ_1 of the total length T of simulation for each system to the long relaxation time τ_1. These ratios may be used to estimate the number of independent samples in the estimates of equilibrium dimensions and autocorrelation functions.

Boundary Condition Effects. The effect of the periodic boundary conditions imposed on the systems was investigated by simulating a system of eight 64-bead chains with a repeat period of 32, rather than 16. This system

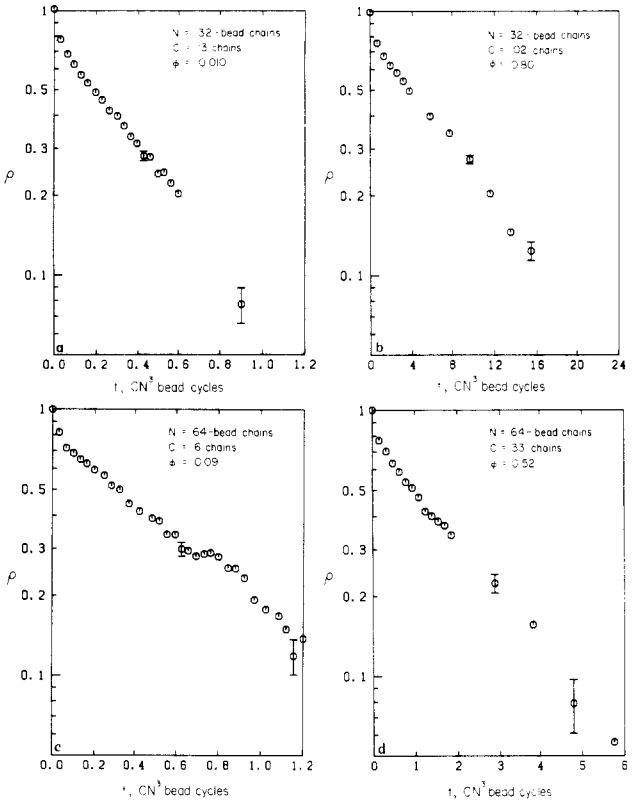

Figure 2. Semilogarithmic plots of autocorrelation functions $\rho(\mathbf{l},\mathbf{l},t)$ for the end-to-end vector $\mathbf{l}$ vs. time t in units of CN^3 bead cycles, for systems of C chains of N beads each occupying fractions $\phi = CN/16^3$ of the lattice sites: (a) $N = 32$, $\phi = 0.010$; (b) $N = 32$, $\phi = 0.80$; (c) $N = 64$, $\phi = 0.09$; (d) $N = 64$, $\phi = 0.52$. The vertical bars shown on selected points extend upward and downward one sample standard deviation of the mean.

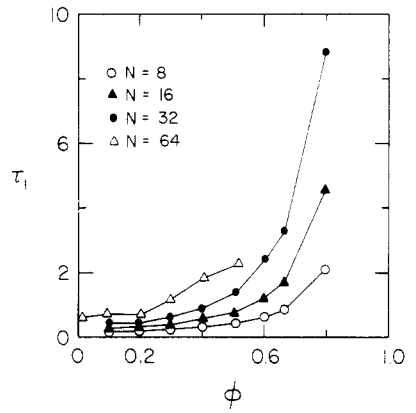

Figure 3. Long relaxation times τ_1 vs. the fraction ϕ of occupied lattice sites for systems of chains of N beads each on a simple cubic lattice.

has the same value of ϕ as the system of one 64-bead chain with a repeat distance of 16, but the repeat volume is eight times as large. The following equilibrium and relaxation properties were obtained (quantities in parentheses are sample standard deviations of the mean): $\langle l^2 \rangle = 152.0$ (2.1); $\langle l^4 \rangle = 33974$ (1140); $a = 0.803$ (0.058); $\tau_1 = 0.524$ (0.056); $D = 8.88$ (0.36). Comparison of these results with those given in Tables I and III for $N = 64$ and $\phi = 0.016$ shows that the differences are less than one standard deviation except for τ_1, where the difference is about 1.5 times the standard deviation for the 8-chain system in a 32-repeat-period space.

Discussion

Figure 3 shows the long relaxation times τ_1 from Table III plotted against ϕ. In the units (CN^3 bead cycles) which

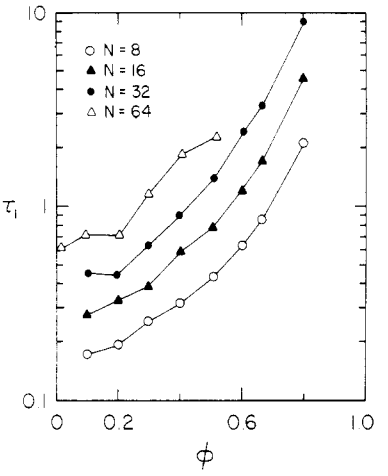

Figure 4. Semilogarithmic plot of the data of Figure 3.

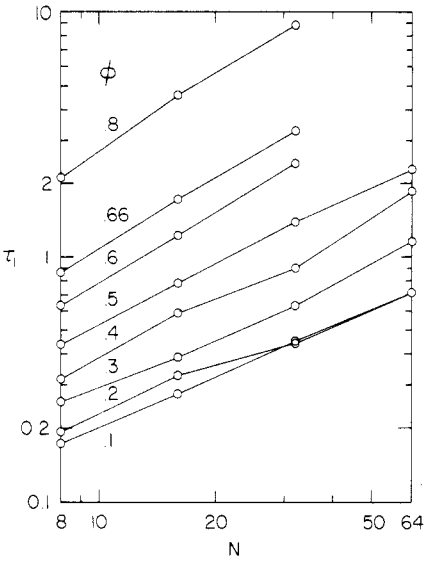

Figure 5. log–log plots of long relaxation times τ_1 vs. N for systems of chains of N beads each as a function of the fraction ϕ of occupied lattice sites.

we have employed here, the relaxation times for a Rouse model or a bead–stick model without excluded volume are essentially independent of chain length except at very short chain lengths. Put another way, the values of τ_1 in these units are proportional to ratios of relaxation times for chains with excluded volume interactions to those for chains of the same length without excluded volume. Thus the chain-length dependences shown here reflect the lengthening of long relaxation times by excluded volume and by inter- and intrachain entanglements. At first glance, the data plotted in Figure 3 appear to suggest an abrupt transition from one type of behavior to another when ϕ reaches the region around 0.6. That this is not the case, however, is shown by Figure 4, which is a semilogarithmic plot of the same data and which shows only a gradual increase in relaxation time with increasing ϕ.

We next consider the dependence of τ_1 upon N at constant ϕ, shown as log–log plots in Figure 5. The data are reasonably consistent with a simple power-law dependence of τ_1 upon N, with the exponent increasing from about 0.7 at $\phi = 0.1$ to about 1.0 at $\phi = 0.8$. A plot of the exponent p vs. ϕ shows roughly linear behavior, though with considerable scatter: $p \simeq g + d\phi$. We therefore extract the N dependence and examine the remaining ϕ dependence by plotting $\tau_1/N^{g+d\phi}$ vs. ϕ, using values $g = 0.57$ and $d = 0.56$, which roughly fit the data shown in Figure 5. The resulting semilogarithmic plot is shown in Figure 6. It will

Table III
Dynamical Data for Chains on a Simple Cubic Lattice[a]

N	ϕ	a	τ_1	D	T_D	T_D/τ_1	$D\tau_1/\langle l^2\rangle$	T/τ_1
8	0.10	0.888 (0.036)	0.172 (0.015)	2.298 (0.069)	0.8	4.6	0.037	55.6
8	0.20	0.900 (0.044)	0.193 (0.016)	1.980 (0.023)	0.8	4.1	0.036	49.8
8	0.30	0.836 (0.018)	0.2554 (0.0069)	1.499 (0.018)	1.2	4.7	0.036	28.2
8	0.40	0.846 (0.015)	0.3159 (0.0078)	1.102 (0.020)	1.2	3.8	0.033	45.6
8	0.51	0.8493 (0.0084)	0.437 (0.015)	0.7619 (0.0076)	1.6	3.7	0.032	22.0
8	0.60	0.8272 (0.0094)	0.631 (0.025)	0.5053 (0.0071)	2.0	3.2	0.032	38.1
8	0.66	0.8201 (0.0073)	0.859 (0.011)	0.3684 (0.0062)	3.6	4.2	0.031	25.2
8	0.80	0.8089 (0.0062)	2.1138 (0.0094)	0.1449 (0.0024)	4.8	2.3	0.031	13.6
16	0.10	0.778 (0.014)	0.276 (0.010)	3.16 (0.22)	1.6	5.8	0.032	139.4
16	0.20	0.780 (0.028)	0.327 (0.014)	2.591 (0.039)	1.6	4.9	0.033	58.7
16	0.30	0.803 (0.014)	0.3878 (0.0055)	2.001 (0.093)	2.0	5.2	0.030	61.9
16	0.40	0.7694 (0.0074)	0.5880 (0.0072)	1.486 (0.072)	1.2	2.0	0.035	24.5
16	0.50	0.7645 (0.0077)	0.778 (0.036)	0.959 (0.013)	2.8	3.6	0.031	21.6
16	0.60	0.783 (0.029)	1.222 (0.012)	0.6301 (0.0078)	2.8	2.3	0.032	13.7
16	0.66	0.772 (0.012)	1.719 (0.062)	0.40524 (0.00052)	4.8	2.8	0.029	16.8
16	0.80	0.800 (0.011)	4.58 (0.27)	0.1410 (0.0050)	7.2	1.6	0.028	9.4
32	0.10	0.756 (0.020)	0.454 (0.017)	4.60 (0.38)	1.2	2.6	0.034	63.5
32	0.20	0.796 (0.020)	0.443 (0.029)	3.43 (0.21)	1.2	2.7	0.026	32.5
32	0.30	0.802 (0.024)	0.632 (0.041)	2.822 (0.065)	2.0	3.2	0.031	38.0
32	0.40	0.775 (0.033)	0.899 (0.079)	1.80 (0.20)	2.4	2.7	0.030	16.0
32	0.51	0.735 (0.021)	1.391 (0.051)	1.140 (0.056)	3.2	2.3	0.030	13.8
32	0.60	0.749 (0.012)	2.417 (0.079)	0.724 (0.040)	6.2	2.6	0.034	15.4
32	0.66	0.754 (0.019)	3.282 (0.207)	0.498 (0.016)	6.9	2.1	0.032	12.6
32	0.80	0.764 (0.022)	8.83 (0.58)	0.1715 (0.0012)	7.7	0.9	0.031	5.2
64	0.016	0.766 (0.039)	0.608 (0.040)	9.06 (0.89)	2.4	3.9	0.036	568.6
64	0.094	0.768 (0.020)	0.716 (0.026)	6.53 (0.76)	2.4	3.4	0.032	80.5
64	0.20	0.830 (0.053)	0.711 (0.070)	4.42 (0.39)	2.8	3.9	0.024	46.9
64	0.30	0.782 (0.050)	1.16 (0.13)	3.46 (0.51)	3.1	2.7	0.034	16.1
64	0.41	0.7362 (0.0057)	1.860 (0.042)	2.22 (0.21)	3.9	2.1	0.033	12.5
64	0.52	0.769 (0.046)	2.28 (0.33)	1.449 (0.092)	3.8	1.7	0.029	10.1

[a] N is the number of beads on each chain, and ϕ is the fraction of lattice sites occupied by beads. The parameters a and τ_1 are determined by fitting the autocorrelation functions $\rho(l,l,t)$ for the end-to-end vector l to the form $a\exp(-t/\tau_1)$ by least squares at time intervals after ρ has decayed below 0.6. D is the translational diffusion constant for the centers of mass of the chains, estimated as $\langle d^2\rangle/(6T_D)$, where $\langle d^2\rangle$ is the mean-square move of the centers of mass of the chains in time T_D. T is the total length of simulation for each system. All times are in units of CN^3 bead cycles, where C is the number of chains per 16^3 lattice sites (i.e., $\phi = CN/16^3$). Quantities in parentheses are sample standard deviations of the mean.

be seen that most of the N dependence has been removed. Thus we can write $\tau_1(N,\phi) = f(\phi)N^{g+d\phi}$. In interpreting the concentration dependence embodied in $f(\phi)$, we turn to the free volume theory.

Free volume has been a widely used and frequently successful concept for describing the long-time dynamical properties of polymer systems.[3,33-35] Assuming that viscosity, dynamic modulus, and long relaxation times all arise in similar ways from the long-time cooperative motions of polymer chains, we might suppose that τ_1 is also governed in part by free volume. According to the free volume picture, the concentration dependence of τ_1 should be given by $\exp(\gamma V^*/V_f)$, where V^* is a volume just large enough to allow a segment to move in, γ is a numerical factor introduced to allow for the possible overlap of free volume between segments, and V_f is the average free volume per segment. In our lattice model, V_f is given by $(1-\phi)/\phi$. Thus we should except to find $f(\phi) = \exp[h + b\phi/(1-\phi)]$, and a semilogarithmic plot of $\tau_1/N^{g+d\phi}$ vs. $\phi/(1-\phi)$ should yield a straight line. The relaxation times in Table III were therefore fitted by least squares to the form

$$\ln \tau_1 = h + b\phi/(1-\phi) + g \ln N + d\phi \ln N \quad (4)$$

The fit gave values $h = -3.095$, $b = 0.464$, $g = 0.570$, and $d = 0.560$. The resulting fit is shown in Figure 7, a semilogarithmic plot of $\tau_1/N^{g+d\phi}$ vs. $\phi/(1-\phi)$. Thus we can summarize the dependence of τ_1 upon chain length and concentration as

$$\tau_1(N,\phi) = e^{h+b\phi/(1-\phi)}N^{g+d\phi} = \tau_1(N,0)e^{b\phi/(1-\phi)}N^{d\phi} \quad (5)$$

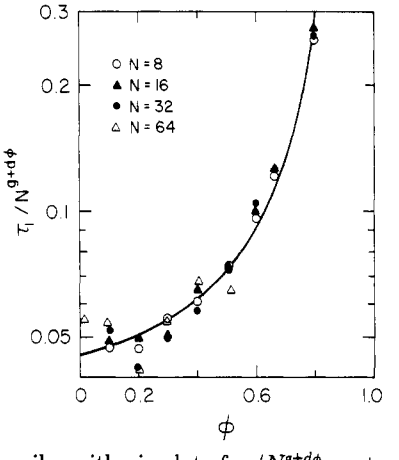

Figure 6. Semilogarithmic plot of $\tau_1/N^{g+d\phi}$ vs. ϕ, where the τ_1 are long relaxation times for systems of N-bead chains on a simple cubic lattice, ϕ is the fraction of occupied lattice sites, and g and d are determined by least squares as described in the text.

where $\tau_1(N,0)$ is, of course, just the dilute-solution relaxation time. Since the units of CN^3 bead cycles in which values of τ are reported here have absorbed the N^2 dependence of relaxation times of chains without excluded volume upon chain length, eq 5 shows that $\tau_1(N,0)$ in "external" units varies approximately as the $2 + g$ or 2.57 power of chain length, in reasonable agreement with the 2.6-power dependence reported in ref 29 for models with two kinds of bead move. According to the last factor in eq 5, as the concentration increases this power dependence

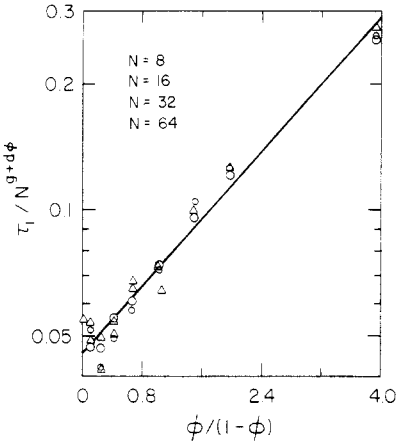

Figure 7. Semilogarithmic plot of $\tau_1/N^{g+d\phi}$ vs. $\phi/(1-\phi)$, where the τ_1 are long relaxation times for systems of N-bead chains on a simple cubic lattice, ϕ is the fraction of occupied lattice sites, and g and d are determined by fitting the data by least squares to the form $\ln \tau_1 = h + d\phi/(1-\phi) + g \ln N + d\phi \ln N$.

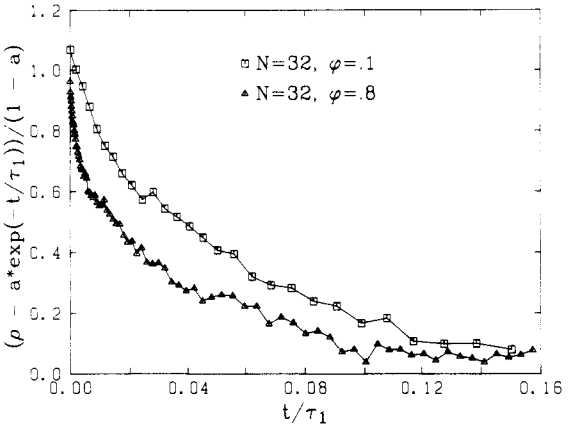

Figure 8. Residual relaxation functions $[\rho - a \exp(-t/\tau_1)]/(1-a)$ vs. t/τ_1, where ρ is the autocorrelation function for the end-to-end vector, with long-time limiting behavior $a \exp(-t/\tau_1)$, for systems of 32-bead chains at low and high values of the fraction ϕ of occupied lattice sites.

increases linearly with ϕ. Thus at least for the range of chain lengths studied in this work, we find no evidence for "crossover" effects from one regime of chain dynamics to another.

Finally, qualitative information about the width of the spectrum of relaxation times may also be extracted from the autocorrelation functions for the end-to-end vector. Although these autocorrelation functions mainly exhibit the longest relaxation time τ_1, they also contain qualitative information about higher relaxation times. If we subtract its long-time limiting behavior $a \exp(-t/\tau_1)$ from a given autocorrelation function, we obtain a "residual" relaxation curve which reflects the contribution of shorter relaxation times to the relaxation of the end-to-end vector. In order to compare the widths of such residual relaxation functions, we divide each by $1 - a$ to obtain values of unity at zero time and scale them to τ_1 by plotting vs. t/τ_1. The resulting curves are shown in Figure 8 for 32-bead chains at the lowest and highest concentrations studied. Plotted in this way, it will be seen that the ratio of the residual relaxation time, however defined, to τ_1 at high concentration is significantly less than its value at low concentration. In other words, the width of the relaxation-time spectrum increases with increasing concentration, in agreement with the analytical treatment of Muthukumar and Freed[36] for dilute solution. Earlier work[27,37] showed that for isolated chains, the intrachain repulsive effects of excluded volume also broaden the relaxation-time spectrum. Thus in this regard, intra- and interchain repulsions have qualitatively similar effects upon the spectrum of relaxation times.

Summary

We have observed the equilibrium dimensions and relaxation behavior of systems of multiple lattice-model polymer chains on a simple cubic lattice. The equilibrium behavior appears to parallel that observed previously by other workers. Autocorrelation functions for end-to-end vector have been obtained for systems of chains of from 8 to 64 beads each, with up to $^4/_5$ the lattice sites occupied by chains. Long relaxation times as a function of chain length and fraction of occupied lattice sites (a measure of concentration) have been inferred from the long-time limiting behavior of the autocorrelation functions. It appears that the dependence of the long relaxation times upon chain length and concentration is reasonably well represented by the combination of a simple free volume effect and an additional chain-length-dependent effect. Qualitatively, increasing the chain concentration appears to broaden the spectrum of relaxation times. The effects of increasing concentration upon the relaxation of the square of end-to-end distance and upon the chain translational diffusion constant are consistent with the concentration dependence of the relaxation of the end-to-end vector. Finally, the ratio $D\tau_1/\langle l^2 \rangle$ relating diffusion constant, longest relaxation time, and equilibrium dimensions appears to be relatively insensitive to concentration.

Acknowledgment. Partial financial support from the Petroleum Research Fund, administered by the American Chemical Society, is gratefully acknowledged. This research was supported in part by the National Resource for Computation in Chemistry under a grant from the National Science Foundation (Grant No. CHE-7721305) and the Basic Energy Sciences Division of the U.S. Department of Energy (Contract No. W-7405-ENG-48). D.E.K. as a visting faculty member thanks Professor Robert Pecora and the Stanford Chemistry Department for providing a most stimulating semester during which a part of this work was accomplished.

References and Notes

(1) Rouse, P. E., Jr. *J. Chem. Phys.* **1953**, *21*, 1272.
(2) Zimm, B. H. *J. Chem. Phys.* **1956**, *24*, 269.
(3) Ferry, J. D. "Viscoelastic Properties of Polymers", 3rd ed.; Wiley: New York, 1980.
(4) Stockmayer, W. H. In "Molecular Fluids"; Balian, R., Weill, G., Eds.; Gordon and Breach: New York, 1976.
(5) de Gennes, P.-G. "Scaling Concepts in Polymer Physics"; Cornell University Press: Ithaca, NY, 1979.
(6) de Gennes, P.-G. *J. Chem. Phys.* **1961**, *55*, 572.
(7) Edwards, S. F.; Grant, J. W. V. *J. Phys. A* **1973**, *A6*, 1169, 1186.
(8) Doi, M.; Edwards, S. F. *J. Chem. Soc., Faraday Trans. 2* **1978**, *74*, 1789, 1818.
(9) de Gennes, P.-G. *Macromolecules* **1976**, *9*, 587, 594.
(10) Klein, J. *Macromolecules* **1978**, *11*, 852.
(11) de Gennes, P.-G. *J. Chem. Phys.* **1980**, *72*, 4756.
(12) DeVos, E.; Bellemans, A. *Macromolecules* **1975**, *8*, 651.
(13) Wall, F. T.; Seitz, W. A. *J. Chem. Phys.* **1977**, *67*, 3722.
(14) Okamoto, H. *J. Chem. Phys.* **1970**, *70*, 1690.
(15) Curro, J. G. *Macromolecules* **1979**, *12*, 463.
(16) Bishop, M.; Ceperley, D.; Frisch, H. L.; Kalos, M. H. *J. Chem. Phys.* **1981**, *75*, 5538.
(17) Olaj, O. F.; Lantschbauer, W. *Makromol. Chem., Rapid Commun.* **1982**, *3*, 847.
(18) Mansfield, M. *J. Chem. Phys.* **1982**, *77*, 1554.
(19) Kranbuehl, D.; Schardt, B. "Computer Modeling of Matter"; American Chemical Society: Washington, D.C., 1978.
(20) Bishop, M.; Ceperley, D.; Frisch, H. L.; Kalos, M. H. *J. Chem. Phys.* **1982**, *76*, 1557.

(21) Baumgärtner, A.; Binder, K. *J. Chem. Phys.* **1981**, *75*, 2994.
(22) Evans, K. E.; Edwards, S. F. *J. Chem. Soc., Faraday Trans. 2*, **1981**, *77*, 1891.
(23) Deutsch, J. *Phys. Rev. Lett.* **1982**, *49*, 926.
(24) Verdier, P. H.; Stockmayer, W. H. *J. Chem. Phys.* **1962**, *36*, 227.
(25) Verdier, P. H.; *J. Chem. Phys.* **1966**, *45*, 2122.
(26) Verdier, P. H. *J. Comp. Phys.* **1969**, *4*, 204.
(27) Kranbuehl, D. E.; Verdier, P. H. *J. Chem. Phys.* **1972**, *56*, 3145.
(28) Kranbuehl, D. E.; Verdier, P. H. *J. Chem. Phys.* **1979**, *71*, 2662.
(29) Kranbuehl, D. E.; Verdier, P. H. *Polym. Prepr., Am. Chem. Soc., Div. Polym. Chem.* **1980**, *21*, 195.
(30) Domb, C.; Fisher, M. E. *Proc. Cambridge Philos. Soc.* **1958**, *54*, 48.
(31) Flory, P. J. *J. Chem. Phys.* **1949**, *17*, 303.
(32) Flory, P. J. "Principles of Polymer Chemistry"; Cornell University Press: Ithaca, NY, 1953.
(33) Doolittle, A. K. *J. Appl. Phys.* **1951**, *22*, 1471.
(34) Cohen, M.; Turnbull, D. *J. Chem. Phys.* **1959**, *31*, 1164.
(35) Cohen, M.; Greist, G. *Phys. Rev.* **1970**, *20*, 1077.
(36) Muthukumar, M.; Freed, K. F. *Macromolecules* **1978**, *11*, 843.
(37) Verdier, P. H. *J. Chem. Phys.* **1973**, *59*, 6119.

Polymer–Cosolvent Systems. 8. Free Volume and Contact Energies in Two Cosolvent Mixtures for Polystyrene and an Interpretation in Terms of a Site Model†

John M. G. Cowie* and Iain J. McEwen

Department of Chemistry, University of Stirling, Stirling FK9 4LA, Scotland.
Received June 20, 1983

ABSTRACT: Cosolvency in the ternary system methylcyclopentane (1) + acetone (2) + polystyrene (3) has been demonstrated by establishing the demixing behavior of the polymer as a function of temperature and solvent composition. Enhanced solvation of the polymer occurs at all intermediate compositions as evidenced by an increased separation of the critical solution temperatures. An analysis of the phase behavior in terms of the free volume theory of polymer solutions reveals that cosolvency has an enthalpic origin, both in this and in a second ternary system acetone (1) + diethyl ether (2) + polystyrene (3). A possible mechanism for cosolvent action by binary liquid mixtures is discussed.

Introduction

The demixing behavior of a polymer dissolved in a binary solvent mixture may be used to study possible cosolvent (or synergistic) action of the liquid pair. If cosolvency occurs the resulting phase diagram will reflect the enhanced solvation of the polymer coil through an increased separation of the demixing temperatures at the upper and lower critical solution temperatures (UCST and LCST). In the case where each of the single liquids is itself a poor solvent, i.e., capable of dissolving only low molecular weight polymers, so-called "classic" cosolvency occurs. In such a system the demixing contours in the composition–temperature plane form a series of closed loops, and examples of this type of behavior are afforded by polystyrene dissolved in mixtures of acetone and diethyl ether[1] and in mixtures of acetone and various *n*-alkanes.[2]

Explanations of cosolvent action in liquid (1) + liquid (2) + polymer (3) systems have been given in terms of an averaging of the solubility parameters δ_1 and δ_2 to a value closer to that of the polymer, δ_3. This implies that $\delta_1 < \delta_3 < \delta_2$, but it has been shown that cosolvency can occur when both δ_1 and δ_2 are greater and smaller than δ_3.[3-5] The modifying effect of a third component on binary systems, in which order may be present, has also been suggested as a possible origin of cosolvent action.[6-8] This may indeed be the case in mixtures which are significantly polar, but it is unlikely in the essentially nonpolar classic systems mentioned above.

Some degree of antipathy between the components of binary cosolvent mixtures has been noted[1,2,4,9] and it has been proposed that unfavorable solvent (1)–solvent (2) contacts may be offset by mutual interaction of the liquids with the polymer and that this will provide the drive for cosolvent action. This concept, through the single-liquid approximation of Scott,[10] has been used as a basis of a semiquantitative description of the acetone (1) + diethyl ether (2) + polystyrene (3) system.[11] However, since polymer–poor solvent contacts must themselves by unfavorable, it is difficult to see this as a complete explanation of cosolvency at the molecular level.

The consequences of unfavorable solvent (1)–solvent (2) interactions have been examined by us, in terms of the Prigogine–Patterson–Flory theory[12,13] of polymer solutions, using a series of cosolvent mixtures for polystyrene formed from acetone and *n*-alkanes ranging from hexane to eicosane.[2] For each of the binary liquid pairs the excess heat of mixing H^E is both large and positive and the mixtures were treated as single fluids whose interaction with the polymer could be characterized by a mixed-solvent interaction parameter χ_{ms}, where

$$\chi_{ms} = \frac{T^* c v^2}{T\tilde{V}} + \frac{c\tau^2}{2(\frac{4}{3}\tilde{V}^{-1/3} - 1)} = \frac{1}{2}(1 + r^{-1/2})^2 \quad (1)$$

with

$$T^* = T\tilde{V}/(1 - \tilde{V}^{-1/3}) \quad (2)$$

and

$$c = p^* V^*/RT^* \quad (3)$$

T^*, p^*, and $V^* = V/\tilde{V}$ are the temperature, pressure, and volume reduction parameters for the solvent mixture and were evaluated according to Flory's theory of binary liquid mixtures.[14] Here, a tilde indicates a reduced quantity. $\tau^2 = (1 - T^*/T_3^*)^2$ quantifies the free volume difference between the polymer (3) and the solvent mixture, and r is the ratio of the hard-core volume of polymer to that of solvent mixture. The free volume difference was found

† Dedicated to Professor W. H. Stockmayer on the occasion of his 70th birthday.

0024-9297/84/2217-0755$01.50/0